Development 139, 1346-1358 (2012) doi:10.1242/dev.076729

Regulation of cranial morphogenesis and cell fate at the neural crest-mesoderm boundary by engrailed 1

Ron A. Deckelbaum[1,*,§], Greg Holmes[2,‡], Zhicheng Zhao[1], Chunxiang Tong[1,*], Claudio Basilico[2] and Cynthia A. Loomis[1,§]

SUMMARY

The characterization of mesenchymal progenitors is central to understanding development, postnatal pathology and evolutionary adaptability. The precise identity of the mesenchymal precursors that generate the coronal suture, an important structural boundary in mammalian skull development, remains unclear. We show in mouse that coronal suture progenitors originate from hedgehog-responsive cephalic paraxial mesoderm (Mes) cells, which migrate rapidly to a supraorbital domain and establish a unidirectional lineage boundary with neural crest (NeuC) mesenchyme. Lineage tracing reveals clonal and stereotypical expansion of supraorbital mesenchymal cells to form the coronal suture between E11.0 and E13.5. We identify engrailed 1 (*En1*) as a necessary regulator of cell movement and NeuC/Mes lineage boundary positioning during coronal suture formation. In addition, we provide genetic evidence that *En1* functions upstream of fibroblast growth factor receptor 2 (*Fgfr2*) in regulating early calvarial osteogenic differentiation, and postulate that it plays an additional role in precluding premature osteogenic conversion of the sutural mesenchyme.

KEY WORDS: Suture, Morphogenesis, Craniosynostosis

INTRODUCTION

In both invertebrates and vertebrates, developmental tissue organization is often achieved by segregation and compartmentalization of morphologically indistinct cell populations that arise from distinct embryonic lineages. Domains encompassing lineage boundaries often harbor regulatory centers that maintain stable compartmental segregation and serve to control cell fate and morphogenesis of evolving structures (Dahmann and Basler, 1999; Irvine and Rauskolb, 2001; Kiecker and Lumsden, 2005). In systems ranging from the *Drosophila* wing disc to the mammalian mid-hindbrain, disruption of boundary integrity results in abnormal development (Dahmann et al., 2011). During vertebrate skull vault (calvaria) development, mesenchymal cells originating from cephalic paraxial mesoderm (Mes) and neural crest (NeuC) lineages largely segregate into caudal and rostral compartments, giving rise to distinct skeletal elements (Couly et al., 1993; Jiang et al., 2002; Evans and Noden, 2006; Yoshida et al., 2008). In mammals, the lineage compartmental interface coincides with the establishment of the coronal suture, which demarcates a physical boundary separating the Mes-derived parietal bone from the apposing NeuC-derived frontal bone (Jiang et al., 2002; Yoshida et al., 2008). The coronal suture constitutes an important growth center for skull development that regulates the proliferation and differentiation rate of osteoprogenitors along the calvarial bone margins (Lenton et al., 2005). Centered within the suture is a mesenchymal population that normally maintains a non-osteogenic fate during embryonic and adult life, but is particularly labile to pathological osseous ablation. The precocious abolishment of this suture, a common form of pediatric craniosynostosis, results in craniofacial deformities associated with increased intracranial pressure and impaired brain and sensory organ function (Morriss-Kay and Wilkie, 2005).

Accumulating evidence from recent studies suggests that regulation of the NeuC/Mes boundary is important to coronal suture development and function. Lesions in *TWIST1* and *MSX2* are causative of human craniosynostosis (Jabs et al., 1993; El Ghouzzi et al., 1997), and these two transcription factors have been shown to cooperate in maintaining the segregation of NeuC-derived osteogenic cells from the Mes-derived sutural mesenchyme in mice (Merrill et al., 2006). Additional mutations in *Jag1* and *Epha4* have further implicated the Notch and receptor tyrosine kinase (RTK) pathways, downstream of *Twist1*, in mitigating inappropriate osteogenic cell migration across the sutural lineage boundary (Ting et al., 2009; Yen et al., 2010). Interestingly, it is still unknown whether activating mutations in the RTK Fgfr2, which are commonly associated with coronal synostosis in Apert syndrome, also lead to disruption of the Mes/NeuC boundary (Wilkie, 1997; Holmes et al., 2009). Although these findings provide a mechanistic framework for investigating the relationship between Mes/NeuC boundary perturbation and craniosynostosis, there is little understanding of the primordial morphogenetic mechanisms responsible for coronal suture formation (prior to E12.5).

Analysis of the *Mesp2* lineage has shown that coronal suture precursors arise within a general population of early gastrulating mesoderm (E6.5-7.5), which additionally contribute to multiple cephalic lineages and cell types including cartilage, vascular endothelium and muscle (Yoshida et al., 2008). Direct labeling of the cephalic mesenchyme at later stages (E13.5) has revealed migratory patterns adopted by supraorbital osteogenic precursors, but failed to mark the coronal suture proper (Yoshida et al., 2008; Ting et al., 2009; Roybal et al., 2010). Although these studies

[1]Department of Pathology and [2]Department of Microbiology, New York University School of Medicine, 550 1st Avenue, New York, NY 10016, USA.

*Present address: Regeneron Pharmaceuticals, 777 Old Saw Mill River Road, Tarrytown, NY 10016, USA
‡Department of Genetics and Genomic Sciences, Mount Sinai School of Medicine, 1428 Madison Avenue, New York, NY 10029, USA
§Authors for correspondence (ron.deckelbaum@regeneron.com; cynthia.loomis@nyumc.org)

Accepted 5 February 2012

suggest the possibility that the suture arises from a distinct non-osteogenic lineage, the precise cephalic location of their precursors remains unknown. Mitigating the inherent limitations of direct labeling techniques, genetic fate-mapping methodologies provide a versatile yet underutilized alternative for investigating the precise origins and morphogenetic behaviors of various mesenchymal populations in the head, including those contributing to coronal suture formation.

Engrailed homeodomain-containing transcription factors participate in regulating lineage boundaries in multiple species and developmental contexts (Araki and Nakamura, 1999; Dahmann and Basler, 2000; Kimmel et al., 2000). We have previously demonstrated a developmental requirement for *En1* in calvarial osteogenesis, and postulated that it plays a role in suture morphogenesis (Deckelbaum et al., 2006). Here we employ inducible genetic fate-mapping strategies to identify the primordial location of coronal suture precursors, and show that these migrate from the paraxial cephalic mesoderm into a supraorbital domain. As suggested in our prior work, *En1* is the earliest known marker expressed in this domain. Using genetic inducible fate mapping, we demonstrate that *En1* is an early transient marker of sutural precursors within the supraorbital domain and provide a morphogenetic model for coronal suture formation that is based on clonal and directional expansion of this precursor population. We also determine that *En1* regulates the distribution of sutural and osteogenic precursors and is required for the positioning and integrity of the Mes/NeuC boundary. Lastly, we illustrate a functional genetic interaction between *En1* and *Fgfr2* in regulating early osteogenic differentiation and suggest an additional role for *En1* in directing the identity of the coronal suture mesenchyme.

MATERIALS AND METHODS

Fate mapping

For fate-mapping studies, *En1-CreER^{T1};R26R* (Sgaier et al., 2005), *Wnt1-CreER^{T1};R26R* (Zervas et al., 2004), *Wnt1-Cre* (Jiang et al., 2002) and *Gli1-CreER^{T2};R26R* (Ahn and Joyner, 2004) males were crossed with outbred Swiss Webster (SW, Taconic) females. For *En1* mutant analysis, mice also carried the *En1^{hd}* or *En1^{lki}* alleles, which encode a homeodomain-deficient (null) form of En1 protein and carry a *lacZ* cassette insertion in exon 1, respectively (Wurst et al., 1994). The morning of vaginal plug detection was designated as E0.5. Females carrying *En1-CreER^{T1};R26R* embryos were administered tamoxifen (TM; 3 mg/20 g body weight; T-5648, Sigma) by oral gavage at E10.5, E11.5 or E12.5. For fate mapping *Wnt1*- and *Gli1*-derived cells, TM was reduced to 1.5 mg/20 g body weight owing to TM-induced lethality at these earlier gestational stages. By inducing recombination in *Gli1-CreER^{T2};R26R* embryos at different time points between E6.5 and E8.5, we determined that optimal labeling in the skull vault is achieved by TM administration at E7.5. Similarly, E7.5 was determined to be the optimal period for inducing *Wnt1-CreER*-mediated recombination in NeuC precursors.

X-Gal staining, in situ hybridization (IHC) and immunohistochemistry

Embryos were prepared for whole-mount detection of β-galactosidase activity and subsequently processed for histological analysis as previously described (Deckelbaum et al., 2006). For embryos older than E15.5, surface ectoderm and superficial dermis were removed to facilitate fixation and staining. In selected specimens, X-Gal staining was followed by Alizarin Red staining of calcified bone. Detection of endogenous alkaline phosphatase activity in tissue sections was performed as previously described (Deckelbaum et al., 2006).

Immunofluorescence was performed on paraffin-embedded sections that were subjected to antigen retrieval (boiled for 35 minutes in 10 mM citrate buffer pH 6.0) using the following primary antibodies: anti-N-cadherin [1:500; MNCD2, Dr M. Takeichi, Developmental Studies Hybridoma Bank (DSHB), University of Iowa]; anti-N-cadherin (1:500; BD Transduction Laboratories, 610920); anti-AP2α (1:50; 3B5, Dr T. Williams, DSHB); anti-cadherin 11 (1:500; Zymed, 71-7600); anti-β-catenin (1:500; Santa Cruz, sc-7199); anti-Pebp2αA (Runx2) (1:100; Santa Cruz, sc-10758); anti-cyclin D1 (1:500; Zymed, 33-3500); anti-β-galactosidase (1:1000; Cappel, 55976); and anti-Fgfr2 (1:100; Santa Cruz, SC-122). Following the reaction with peroxidase-conjugated secondary antibodies (1:250; Jackson ImmunoResearch, 111-035-006), signal amplification was achieved by catalyzed reporter deposition (CARD) of biotinylated tyramide and the subsequent coupling to streptavidin-conjugated Alexa Fluor 488 as previously described (Hopman et al., 1998; Speel et al., 1999).

ISH on whole-mount embryos and paraffin-embedded sections was performed as previously described (Deckelbaum et al., 2006). Fluorescent signal detection was obtained with Fast Red (Sigma) under 594 nm excitation.

RESULTS

The coronal suture originates from hedgehog-responsive cells within the cephalic paraxial mesoderm

To investigate whether cranial bone and suture progenitors localize to certain cephalic mesodermal compartments we first searched for suitable molecular markers that would be activated prior to overt calvarial development. In agreement with prior reports (Echelard et al., 1993; Hui et al., 1994), cephalic expression of sonic hedgehog (*Shh*), a member of the hedgehog (Hh) family of secreted morphogens, localizes to the notochord and prechordal plate between E7.5 and E8.5 (Fig. 1A-C). By comparison, cells expressing the Hh target gene *Gli1* are present in the paraxial Mes, immediately flanking the ventral neural tube, as well as in the neural tube itself (Fig. 1D-F). Notably, this *Gli1*-positive mesenchyme is likely to comprise only a small subpopulation of the cephalic Mes (Yoshida et al., 2008).

We next evaluated the precise spatial and temporal distribution of the Hh-responsive *Gli1^{+}* lineage utilizing an inducible genetic fate-mapping approach, employing the *Gli1-CreER^{T2}* and *R26R* (*lacZ*) reporter alleles (Fig. 2A) (Soriano, 1999; Ahn and Joyner, 2004). Following a single dose of 4-hydroxytamoxifen (TM) at E7.5 to induce Cre-mediated recombination and permanent reporter activation, *Gli1-CreER^{T2}*-marked mesenchymal cells have relocated ventrally and ventrolaterally to the mesencephalon and diencephalon by E9.5 (Fig. 2B, supplementary material Fig. S1A,B). In addition, *Gli1*-derived cells are observed above the developing eye (Fig. 2B, arrowhead). By contrast, NeuC-derived mesenchyme largely occupies rostral aspects of the head by E9.5, as demonstrated by both *Wnt1-CreER^{T1}*-mediated fate mapping and immunodetection of the neural crest marker AP2α (Tfap2α – Mouse Genome Informatics), consistent with prior studies (Fig. 2C, supplementary material Fig. S1C,D) (Shen et al., 1997).

Consistent with these whole-mount studies, analysis of coronally sectioned heads by β-gal/AP2α immunofluorescence 30 hours following TM injection at E7.5 shows a proportion of *Gli1-CreER^{T2}*-derived mesenchymal cells located adjacent to ectocranial NeuC mesenchyme at E8.5 (Fig. 2D-G) and juxtaposed in the supraorbital region by E9.0 (Fig. 2H). None of the *Gli1-CreER^{T2}*-marked cells expresses the NeuC marker AP2α, validating the Mes origin of these cells (Fig. 2D-H; *n*=4 embryos). Definitive analysis of the *Gli1-CreER^{T2}*-derived mesenchyme between E11.5 and P0 demonstrates that these paraxial progenitors give rise to the coronal suture and significantly contribute to the parietal bone (Fig. 2I-M, supplementary material Fig. S2). Additional *Gli1-CreER^{T2}* progeny are detected in other tissues of putative Mes origin, including the lambdoid suture, interparietal bone, supercilliary dermis, and

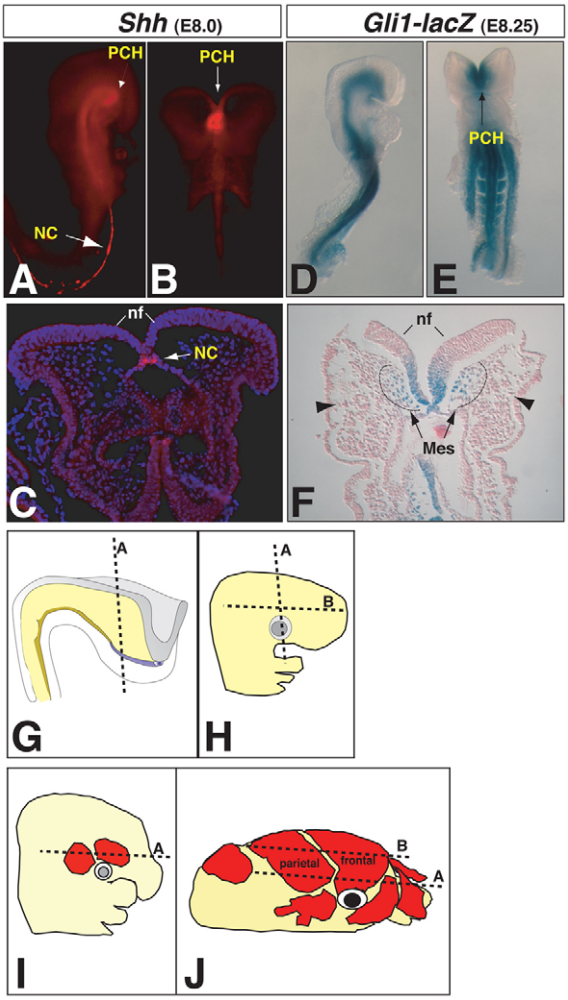

Fig. 1. Hh-responsive cells in the cephalic paraxial mesoderm E8. (**A-C**) Whole-mount and section in situ hybridization (ISH) analysis showing expression of *Shh* (red) throughout the entire extent of the developing mouse notochord (NC), reaching its rostral limits within the prechordal plate (PCH) at E8.0. C is counterstained with eosin. (**D-F**) *Gli1-lacZ* reporter analysis identifies hedgehog (Hh)-responsive cells in the paraxial cephalic Mes (blue), bilaterally flanking the ventral neural tube and PCH at E8.5 (F, arrows). *Gli1*$^{+}$ cells are also present in the ventral neural tube, but are not detected in the presumptive NeuC-derived cephalic mesenchyme (F, arrowheads). (**G-J**) Planes of section in this (as shown in G) and other figures. Skeletal primordial are indicated in red. nf, neural folds.

occipital and tympanic cartilages (Fig. 2K, supplementary material Fig. S3). We therefore conclude that coronal suture precursors originate from *Shh*-responsive cells in the paraxial cephalic mesoderm at E7.5-8.0. Remarkably, these cells migrate rapidly from their original paraxial positions to accumulate within a supraorbital domain of the ectocranium (E8.5-9.5), prior to giving rise to the coronal suture and the juxtaposed ossifying tissues (Fig. 2P).

The coronal suture demarcates a compartmental boundary for neural crest but not the mesodermal lineage

Although our data confirm a generalized segregation of NeuC and Mes lineages in the ectocranial mesenchyme (supplementary material Fig. S1), in agreement with previous reports (Chai et al., 2000), an unexpected proportion of *Gli1-CreER*^{T2}-marked cells consistently intermingles with AP2α-positive cells above the optic placode at E9.0 (Fig. 2H). Analysis at later stages indicates that these *Gli1* progeny assume an osteogenic fate within the frontal bone mesenchyme by E13.5 (supplementary material Fig. S2C,D), which later give rise to osteoblasts that are detected throughout the caudal and basocaudal aspects of the frontal bone proper (Fig. 2L-N). Although we detected *Gli1*-derived cells along the entire basal-apical axis of the frontal bone juxtaposing the coronal suture (Fig. 2L, black arrow, yellow arrowheads; Fig. 2M, yellow arrowheads), a larger population was evident within the basal portion of this rudiment (Fig. 2L, yellow arrow). Analysis of calvarial sections from mice expressing *Mesp2-Cre*, an established driver allele in primordial embryonic mesoderm (Yoshida et al., 2008), confirms that Mes-derived osteoblasts integrate into the developing frontal bone (Fig. 2O). Conversely, progeny of *Wnt1-Cre*-derived NeuC are never detected in the coronal suture mesenchyme or parietal bone (see below).

Our data therefore demonstrate that the mammalian calvarial Mes/NeuC boundary is more complex than originally described (Jiang et al., 2002; Yoshida et al., 2008) and is unidirectional by nature; the Mes compartment (coronal suture mesenchyme and parietal bone) remains impervious to NeuC, while the postulated NeuC-derived compartment (frontal bone) allows for lineage intermingling (Fig. 2O).

The coronal suture is clonally derived from *En1*$^{+}$ cells originating within the supraorbital domain

Based on our observations, we reasoned that early coronal suture and cranial bone development is morphogenetically regulated within the supraorbital domain. In support of this postulate, we observed that primordial cephalic osteoblastic commitment, as determined by analyses of *Runx2* and *Osx* (*Sp7* – Mouse Genome Informatics) mRNA and protein expression, initiates within the supraorbital mesenchyme between E12.0 and E13.5 (Fig. 3A-F). Moreover, a number of transcription factors known for their roles in calvarial development – *Msx2*, *Twist1* and *En1* – are precisely activated within this domain at even earlier stages (Fig. 3G-P, Fig. 4A-H).

To directly evaluate the fate and morphogenetic behavior of this skeletogenic population we focused on *En1*, one of the first known markers expressed across this unique region (Deckelbaum et al., 2006). Detailed examination of primordial *En1* activation revealed that *En1* mRNA remains focally restricted to a region immediately above the eye (Fig. 4A-D, arrowheads). By contrast, the well-characterized *En1-lacZ* reporter exhibits an apically expanded staining pattern (Fig. 4E-H). These distinctions become further pronounced between E12.5 and E13.5. Given the expanded region of cells retaining β-gal activity compared with the spatially restricted *En1* mRNA, β-gal perdurance is likely to act as a transient lineage tracer, depicting the movement and growth of cells beyond the limits of the supraorbital domain.

To directly evaluate the fate and morphogenetic behavior of the supraorbital population, we sought to indelibly mark the earliest *En1*-expressing cells at E11.0 using an inducible *En1-CreER*^{T1} knock-in allele (Sgaier et al., 2005) and then to follow the tagged progeny during successive stages of skull development. Consistent with *En1* initiation at E11.0, we determined E10.5 as the earliest time point for inducing efficient labeling of supraorbital cells (Fig. 4I-K,N); no labeling of this population is detected following injections at E9.5, compatible with a 24-hour clearance period for TM (Kimmel et al., 2000; Zervas et al., 2004), (Fig. 4L,M).

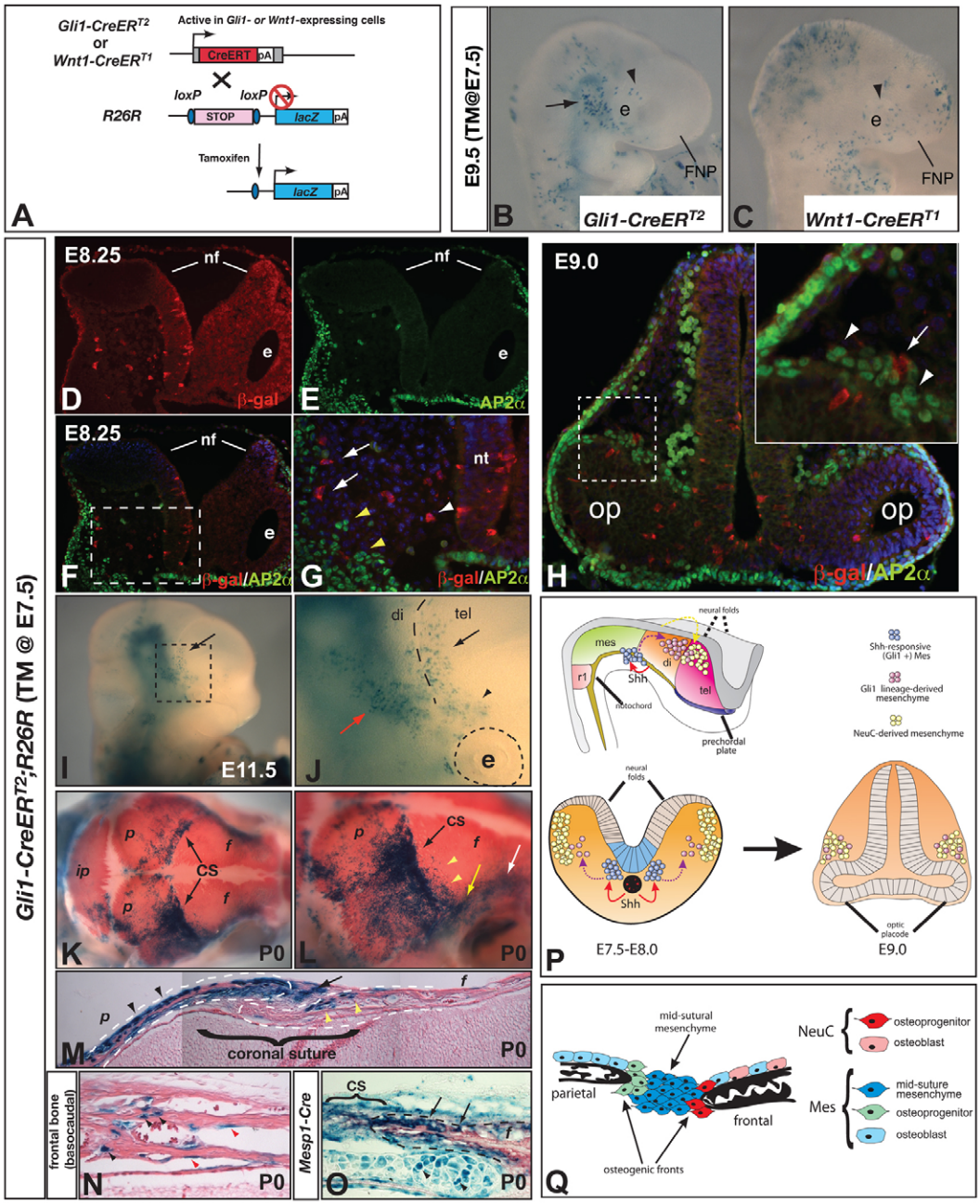

Fig. 2. Hedgehog-responsive cells of paraxial Mes give rise to the coronal suture. (**A**) Inducible genetic fate-mapping strategy for indelibly marking *Gli1*- or *Wnt1*-expressing cells. (**B**,**C**) β-gal staining in *Gli1-CreER^{T2};R26R* and *Wnt1-CreER^{T1};R26R* embryos at E9.5 following tamoxifen (TM) administration at E7.5. Note prominent *Gli1-CreER^{T2}*-mediated labeling in cephalic mesoderm underlying the diencephalon (arrow, B) and *Wnt1-CreER^{T1}*-mediated labeling in the frontonasal process (FNP); both embryos exhibit labeling in the supraorbital region (arrowheads). (**D-G**) Simultaneous immunodetection of *Gli1-CreER^{T2}*-derived (β-gal, red) and NeuC-derived (AP2α, green) mesenchyme at ~E8.5 on coronally sectioned head (the plane of section is that shown in Fig. 1G; owing to the oblique angle, the left side is immediately posterior to the eye). *Gli1*-derived mesoderm juxtaposes the neural tube (G, white arrowhead) and approximates NeuC mesenchyme (yellow arrowheads) within the ectocephalic domain (arrows). The boxed region in F is magnified in G. (**H**) At E9.0, *Gli1-CreER^{T2}*-derived cells (arrow) intermingle with NeuC above the optic placode (arrowheads) (the plane of section is A in Fig. 1H). (**I**,**J**) *Gli1-CreER^{T2}*-derived mesenchyme localizes to the supraorbital domain at E11.5 (arrowhead), giving rise to a population that extends apically along the diencephalic-telencephalic boundary (black arrow). Additional labeling is observed more posteriorly, in putative parietal bone and dermal precursors (red arrow). The boxed region in I is magnified in J. (**K-N**) *Gli1-CreER^{T2}* lineage labeling in the skull vault at P0 showing prominent staining throughout the coronal suture (CS), including the mid-sutural mesenchyme (arrow, M) and in parietal bone osteoblasts (black arrowheads, M). Additional labeling is observed in interparietal and frontal bone osteoblasts (M, yellow arrowheads; N, red arrowheads) and osteocytes (N, black arrowheads) (section planes are A and B in Fig. 1J). (**O**) *lacZ*-labeled frontal bone osteoblasts near the coronal suture of *Mesp1-Cre;R26R* newborn mice (section plane is A in Fig. 1J). (**P**) Schematic depicting the migration of Hh-responsive cells from the paraxial Mes at E7.5 (blue) to relocate laterally by E8.5 (purple), where some intermingle with NeuC cells (yellow) above the developing eye. (**Q**) Modified model of coronal Mes/NeuC lineage compartmentalization showing unidirectional crossing of Mes derivatives into the frontal bone (PB). di, diencephalon; tel, telencephalon; e, eye; nt, neural tube; op, optic placode; r1, rhombomere 1; f, frontal bone; p, parietal bone; ip, interparietal bone.

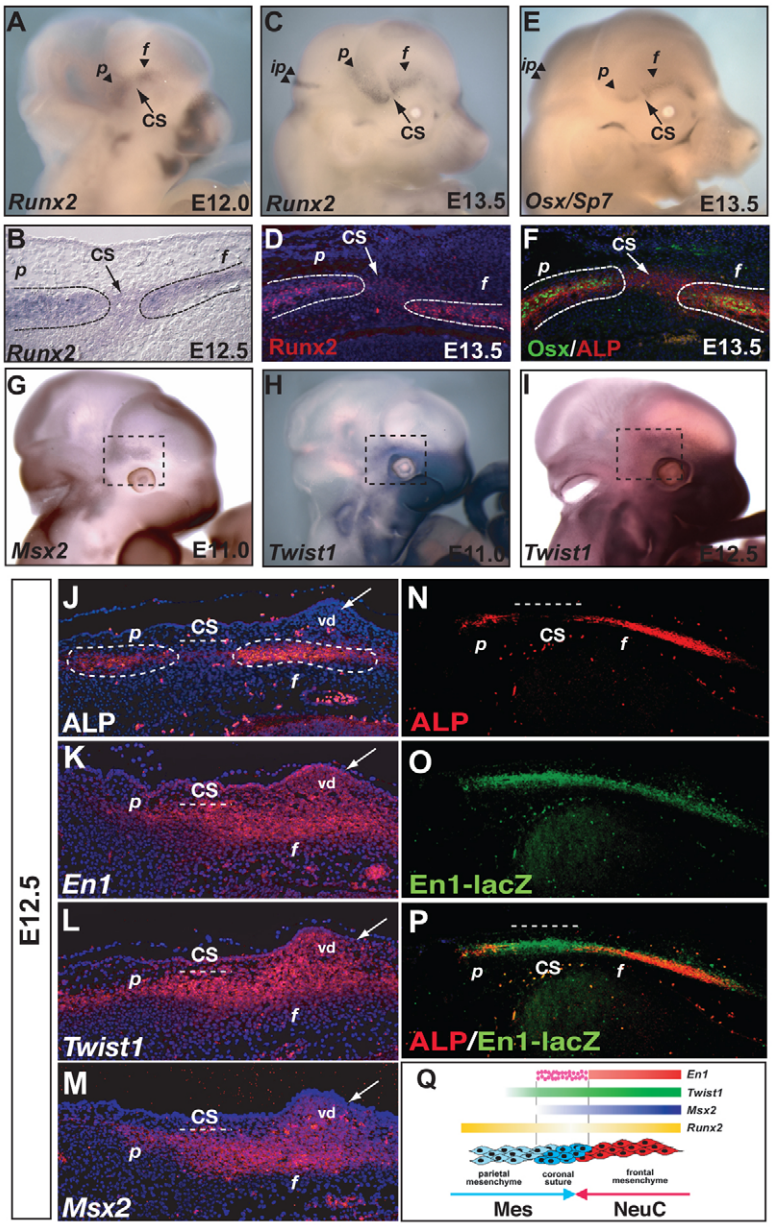

Fig. 3. Expression of osteogenic determinants and molecular regulators of coronal suture development during early cranial development (E11.5-13.5). (**A**,**B**) Whole-mount and section mRNA ISH analysis showing that initiation of cephalic expression of *Runx2* marks the prospective parietal and frontal bone osteogenic populations within the supraorbital domain at E12.5. Note low levels of *Runx2* mRNA within the prospective coronal suture (B, arrow CS). (**C**) Expression of *Runx2* in parietal/frontal bone osteoprogenitors expands apically from their initial supraorbital locale by E13.5 (arrowheads). (**D**) Immunodetection of high levels of Runx2 protein in parietal/frontal bone (p,f, dashed line) osteoprogenitors, and low levels within the coronal suture mesenchyme at E13.5 (arrow CS). (**E**) Expression of Osx lags behind that of Runx2 and is restricted to the supraorbital domain at E13.5 (arrowheads). (**F**) Transverse sections of E13.5 heads show the apposition of ALP$^+$/Osx$^+$ osteogenic populations marking the frontal-parietal bone primordia. The prospective coronal suture exhibits a complete absence of Osx (arrows). (**G-M**) Localization of *Msx2*, *Twist1* and *En1* mRNA to the supraorbital domain in whole-mount embryos (G-I, dashed boxes) or transverse sections of the head (J-M) between E11.0 and E12.5. At this developmental stage, the markers are expressed in both dermal and deeper calvarial progenitors (K-M). Relative to cephalic osteogenic populations (J, ALP$^+$), *En1*, *Msx2* and *Twist1* exhibit overlapping expression with the prospective frontal bone and coronal suture domains, and *Twist1* also extends further caudally into the parietal domain (K-M). (**N-P**) Simultaneous detection of ALP (red) and *En1-lacZ* reporter activity (anti-β-galactosidase, green) at E12.5 shows overlapping expression in the prospective frontal bone and edge of the parietal bone; only *En1-lacZ* is expressed in the coronal suture. (**Q**) Schematic summary depicting the spatial relationship of regulatory gene expression to the primordial skeletogenic populations (and their respective lineage assignments) within the supraorbital domain. Section plane as in Fig. 1I. vd, vibrissa dermis; ALP, alkaline phosphatase activity.

Temporal analysis of the *En1* lineage reveals a stereotypically patterned distribution of two populations emanating from their supraorbital point of origin. The more caudal population rapidly extends towards the head vertex, forming a narrow band during E12.5-13.5 (Fig. 4I,J, arrowheads). Detailed analysis at E16.5 confirms that these cells ultimately give rise to the entire extent of the coronal suture, as evidenced by prominent marking of mid-sutural mesenchyme and cells within the flanking frontal/parietal bone margins (Fig. 4K,N,O). By comparison, a second population progressively extends rostrally, remaining closely associated with the supraorbital region between E12.5 and E13.5 (Fig. 4I,J, arrows), and later gives rise to the basal portion of the frontal bone (Fig. 4K,N,O). In addition to these primary trajectories, *En1*-derived cells exhibit secondary morphogenetic patterns, suggested by caudal-rostral and basal-apical *lacZ* staining gradients detected in the parietal and frontal bones, respectively. Interestingly, TM administration at later time points (E11.5 or E12.5) results in significant and progressive reduction in coronal suture labeling (Fig. 4P-U), suggesting that by E11.5 most sutural precursors have already relocated to positions apical to the *En1* expression domain. We therefore conclude that the coronal suture arises from cells transiently expressing *En1*, which clonally expand and migrate apically from their supraorbital point of origin.

En1 regulates the positioning of the calvarial Mes/NeuC lineage boundary

We next asked whether *En1* plays a regulatory role in morphogenetic events ascribed to the supraorbital domain and whether this might underlie the distinct coronal suture anomalies we had previously reported in *En1* mutants (Deckelbaum et al., 2006). As both *Drosophila engrailed* and mammalian *En1* play well-established roles in restricting cell movement along compartmental boundaries (Blair and Ralston, 1997; Hanks et al., 1998; Dahmann and Basler, 1999; Dahmann and Basler, 2000; Kimmel et al., 2000), we hypothesized that *En1* might play an analogous function in regulating the Mes/NeuC lineage boundary.

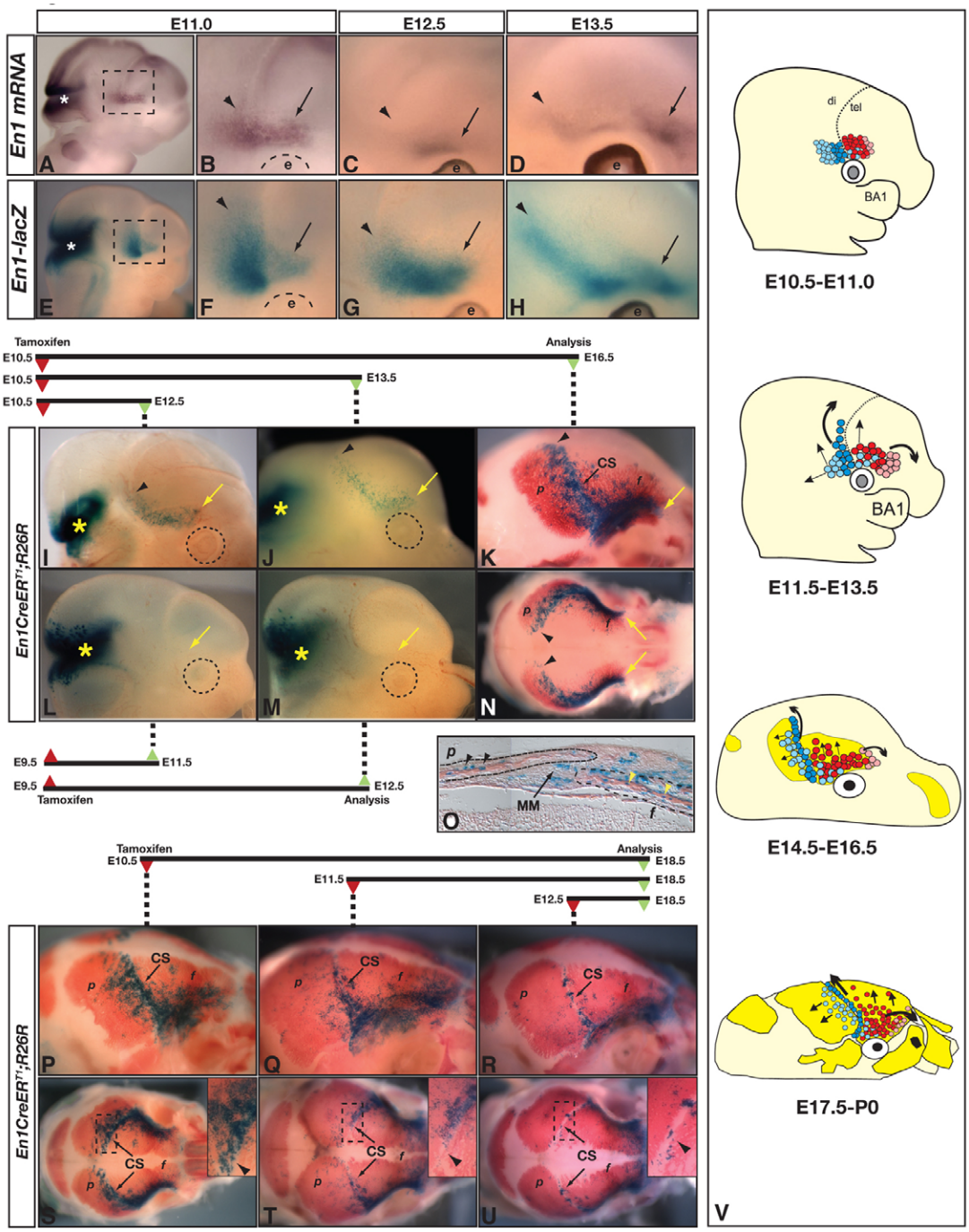

Fig. 4. Coronal suture precursors arise from supraorbital *En1*-expressing cells at E11.0. (**A-H**) Analysis of supraorbital *En1* expression by *lacZ* reporter activity or RNA ISH between E11.0 and E13.5, showing the relative expansion of the caudal *En1-lacZ* domain (arrowheads) compared with the two overlapping rostral domains. Asterisk indicates expression in the mid-hindbrain. Note that the apparent arc-shaped staining along the telencephalon boundary in B is due to probe trapping. (**I-K**,**N**,**O**) The *En1-CreER*-derived cephalic lineage observed between E12.5 and E16.5 following TM administration at E10.5. Labeling progressively extends from the supraorbital domain (arrows) apically (E12.5-13.5), ultimately marking the entire extent of the coronal suture (E16.5). Histological analysis confirms labeling in sutural mesenchyme (O, MM arrow) and flanking parietal-frontal bones (O, arrowheads) (section plane A in Fig. 1J). In addition, *En1*-derived cells are observed along the entire base of the frontal bone (yellow arrows) and the rostral portion of the parietal bone, with reduced labeling in regions distant from these axes. (**L**,**M**) As anticipated, no *En1-CreER*-derived cells are detected in the calvaria between E11.5 and E12.5 when TM is administered at E9.5, despite high recombination levels in the mid-hindbrain (asterisk; also compare with I,J). (**P-U**) TM administration at E10.5 (P,S), E11.5 (Q,T) and E12.5 (R,U), showing a progressive decline in the extent of *En1-CreER* labeling in the coronal suture, particularly near the apex (insets, arrowheads). (**V**) Model for coronal suture and adjacent bone formation from the supraorbital domain. *En1* expression at E11.0 traverses a population encompassing Mes-derived coronal suture (blue), parietal and frontal bone progenitors (light blue), in addition to NeuC-derived frontal bone progenitors (red and pink). Between E11.5 and E13.5, coronal suture precursors migrate apically to the supraorbital domain, while frontal bone progenitors extend rostrally (large arrows). This growth pattern prefigures the coronal suture and establishes an orthogonal relationship between coronal suture and frontal bone formation (large arrows, E14.5-P0). Secondarily, parietal and frontal bone growth proceeds at right angles to these primary axes (small arrows). BA1, first branchial arch.

Consistent with a general role for *En1* in restricting cell movement, *En1*-null mouse embryos exhibit aberrant apical scattering of *En1-CreER*^{T1}-labeled cells, and this is particularly pronounced in the NeuC population (Fig. 5A,B). Similarly, examination of the Mes or NeuC lineage in *En1* mutants indicated aberrant cell positioning along the coronal suture boundary. In agreement with prior studies (Jiang et al., 2002; Merrill et al., 2006), analysis of *Wnt1-Cre*-labeled NeuC in wild-type embryos confirms that this lineage is strictly confined to the frontal bone and its primordia (Fig. 5C,E,G, supplementary material Fig. S4A). Remarkably, *En1*$^{-/-}$ littermates exhibit a generalized caudal shift in the position of the skeletogenic NeuC lineage boundary at E15.5, visible on whole-mounts as a transformation from a normal chevron-shaped to an arc-shaped caudal border (Fig. 5C,D). Histological analysis of E15.5 calvaria reveals an ectopic extension of *Wnt1-Cre* descendants into the coronal mid-sutural mesenchyme of *En1* mutants (Fig. 5E,F). Moreover, a caudal expansion of the NeuC domain is visible in mutant embryos as early as E12.5 (Fig. 5G,H). Conversely, there is a substantial reduction in *Gli1-CreER*^{T2} progeny in the coronal suture of *En1* mutants (Fig. 5I,J, supplementary material Fig. S4C,D; observed in 9/14 sutures), indicating that caudal expansion of NeuC occurs at the expense of Mes. Notably, we found evidence for ectopic invasion of NeuC derivatives within the parietal bone of *En1* mutants at later developmental stages (supplementary material Fig. S4B; observed in 5/7 sutures), indicating a secondary role for *En1* in maintenance of Mes/NeuC boundary integrity. Consistent with this phenotype, the activity of *Msx2* and *Twist1*, which are synergistic regulators of the Mes/NeuC boundary and coronal suture integrity (Merrill et al., 2006; Ting et al., 2009), is altered in *En1* mutants at E12.5. Specifically, *Msx2* expression aberrantly extends caudally beyond the prospective coronal suture boundary, while *Twist1* is diminished in this zone and remains downregulated later in development (Fig. 5K-P).

In summary, precise regulation of *En1* expression is required to produce the narrowly focused apical stream of Mes-derived cells that forms the coronal suture. In the absence of early *En1*

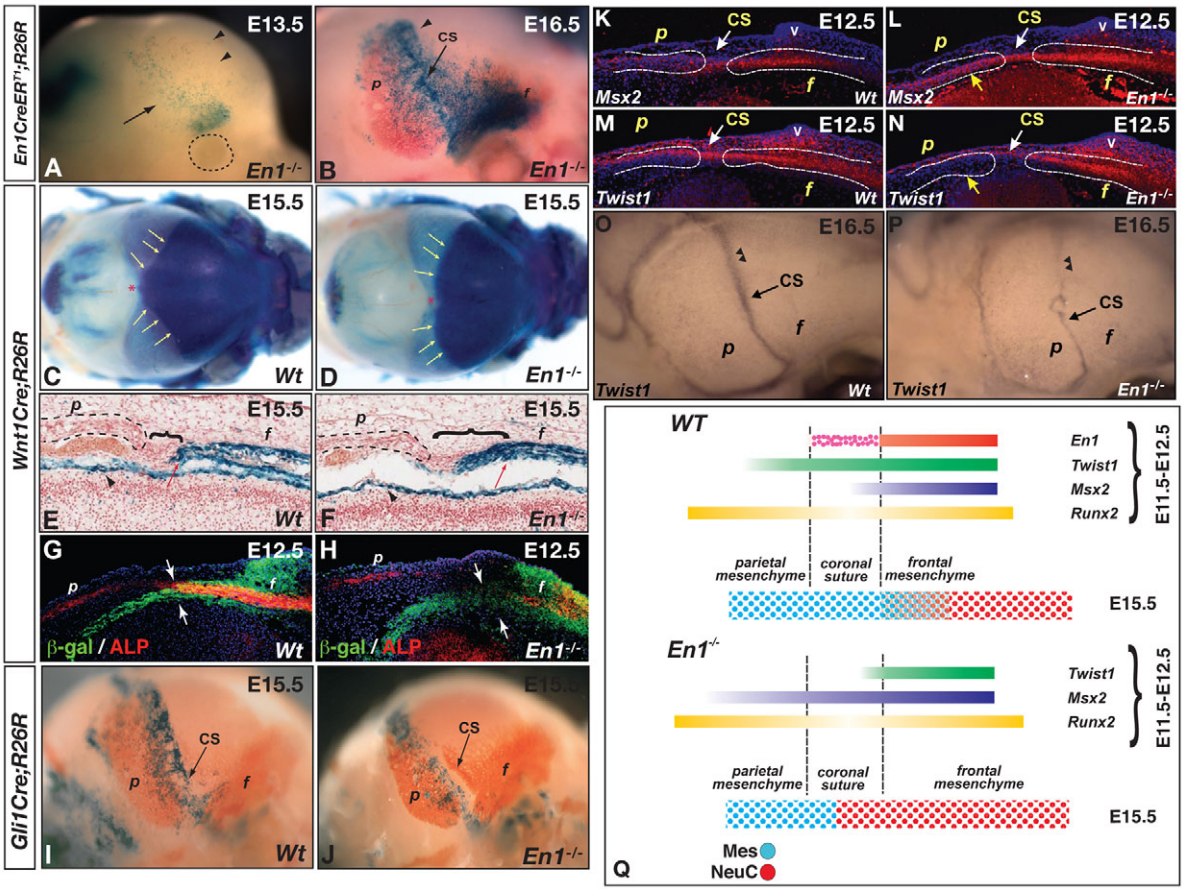

Fig. 5. *En1* regulates the coronal Mes-NeuC lineage boundary. (**A**,**B**) *En1-CreER*-mediated lineage tracing in *En1*-null mutants shows aberrant distribution of calvarial labeling at E13.5 (A) and E16.5 (B). (**C-F**) NeuC lineage tracing via *Wnt1-Cre;R26R* at E15.5 shows that *En1*$^{-/-}$ embryos, by comparison with wild-type embryos, exhibit a caudal shift in the coronal NeuC lineage boundary (yellow arrows in C,D), which histologically presents as an ectopic NeuC extension into the coronal suture mid-sutural mesenchyme (E,F, brackets). No difference in labeling of the dura mater is observed between wild-type and *En1* mutants (arrowheads) (section plane as B in Fig. 1J). Asterisk, skull apex. (**G**,**H**) Immunodetection of the *Wnt1*-Cre lineage (green) with respect to primordial frontal (f) and parietal (p) bone osteogenic populations (ALP, red) at E12.0, showing a caudal expansion of *Wnt1-Cre*-derived cells in *En1* mutants (arrows) (section plane as Fig. 1I). (**I**,**J**) *Gli1-CreER*^{T2}-mediated tracing shows a reduction in labeling within the coronal suture of *En1*-null mutants at E15.5. (**K-N**) ISH analysis on transverse section of E12.5 embryos shows that *En1*-null mutants exhibit upregulation and caudal expansion of *Msx2*, which traverses the primordial suture and parietal bone (FB-PB) domain, whereas *Twist1* expression is reduced in the prospective coronal suture (section plane as Fig. 1I). (**O**,**P**) *En1* mutants continue to display reduced *Twist1* expression in the coronal suture at E16.5. (**Q**) Summary of cM/cNC boundary perturbation and associated alterations in regulatory gene expression observed in the supraorbital domain of *En1* mutants. v, vibrissa.

expression, fewer Mes cells contribute to the forming suture and their expression of crucial transcription factors is significantly altered. Concomitantly, *En1*-negative NeuC cells exhibit precocious and exacerbated apical migration and aberrant infiltration into the coronal sutural territory (Fig. 5Q), processes that result in a caudally shifted Mes/NeuC boundary and a widened dysmorphic suture (supplementary material Fig. S5).

En1 and *Fgfr2* cooperate to regulate calvarial osteogenic differentiation and coronal suture morphogenesis

In light of its role in suture morphogenesis and calvarial bone differentiation, we next sought to investigate whether *En1* might also affect or interact with molecular pathways known to regulate these processes. It is well established that tight modulation of Fgfr2 signaling is vital to both coronal suture patency and calvarial osteoblastic differentiation. Following from our previous studies (Deckelbaum et al., 2006), we noted that *Fgfr2* expression levels are dysregulated in the coronal sutures of *En1* mutants (supplementary material Fig. S6A,B). Likewise, coronal sutures of *En1*-null embryos exhibit reduced levels of the Fgfr2 target genes *Dusp6* and *Spry2* (supplementary material Fig. S6C-F) (Hanafusa et al., 2002; Li et al., 2007), as well as diminished levels of *Twist1* (Fig. 5M,N), which functions upstream of *Fgfr2* in regulating coronal suture closure (Rice et al., 2000; Connerney et al., 2006; Connerney et al., 2008). Thus, both regulators and targets of the Fgf pathway are anomalously expressed in *En1* mutants.

To evaluate the functional importance of altered Fgf signaling, we utilized a well-established murine model for human Apert (AP) syndrome. Mice harboring an inducible allele designed to express a gain-of-function mutant form of Fgfr2 ($Fgfr2^{S252W}$, denoted $Fgfr2^{AP}$ henceforth), develop predictable prenatal coronal synostosis (Chen et al., 2003; Holmes et al., 2009). As a first step, we generated mice designed to selectively induce expression of $Fgfr2^{AP}$ within the *En1-Cre* lineage ($En1^{Cre/+};Fgfr2^{AP}$) (supplementary material Fig. S7), which, according to our fate-mapping analysis, would be predicted to initiate within the primordial coronal suture at E11.0. This experimental strategy circumvents the possibility of targeting skeletogenic populations that do not express *En1*, thereby allowing us to address the long-standing question of whether Fgfr2 activation in the cranial base is a primary, albeit indirect, cause of coronal synostosis in AP syndrome (Wang et al., 2005; Nagata et al., 2010). Analysis of $En1^{Cre/+};Fgfr2^{AP}$ mutants at embryonic and postnatal stages confirms that all affected mice exhibit hallmark AP features (Chen et al., 2003; Wang et al., 2005; Holmes et al., 2009), including coronal synostosis, pronounced midfacial hypoplasia, and malocclusion developing between E15.5 and P0 (Fig. 6, supplementary material Fig. S7 and Table S1). Our data therefore demonstrate that restricted activation of *Fgfr2* within *En1*-expressing neurocranial populations, and not in cells of the cranial base, is sufficient for full manifestation of the cranial AP phenotype.

To test our hypothesis that diminished Fgf signaling is partially causative of the *En1* mutant calvarial phenotype, we generated *En1*-null;$Fgfr2^{AP}$ compound mutants by combining two *En1*-null alleles [$En1^{Cre}$ and $En1^{lki}$ (*lacZ* knock-in); supplementary material Fig. S7] with the Apert allele, and asked whether expression of activated Fgfr2 would rescue the osteogenic and coronal suture phenotypes resulting from *En1* deficiency. As previously shown (Deckelbaum et al., 2006), *En1* mutants exhibit reduced frontal bone ossification due to perturbed osteoblastic differentiation (Fig. 7D, asterisk). Activation of the $Fgfr2^{AP}$ allele in the *En1*-null background ($En1^{Cre/lki};Fgfr2^{AP}$) results in a fully penetrant augmentation of calvarial bone formation, evidenced by apical expansion of the frontal bone and increased alkaline phosphatase activity (ALP; ALPL – Mouse Genome Informatics) expression by E15.5 (compare Fig. 7B,B′ with 7D,D′). Moreover, preceding overt bone formation, activated $Fgfr2^{AP}$ results in strong upregulation of Runx2 and rescues the delay in Osx initiation within osteogenic precursors of *En1* mutants at E12.5 (Fig. 7F,L, supplementary material Fig. S8B,D). Importantly, expression of Fgfr2 protein, which is otherwise reduced in osteogenic cells of *En1* mutants (Fig. 7I,J), is restored to normal levels in $En1^{Cre/lki};Fgfr2^{AP}$ calvarial rudiments (Fig. 7P). We thus identify a crucial role for *En1* in regulating *Fgfr2*-mediated calvarial osteogenic differentiation.

Unexpectedly, our analyses uncovered a more complex regulatory relationship during suture morphogenesis. As demonstrated in our previous studies (Deckelbaum et al., 2006), *En1*-null ($Fgfr2^{+/+}$) calvaria reveal exaggerated coronal suture patency and dysmorphology when compared with wild-type or *En1* heterozygous embryos at both E15.5 and P0 (Fig. 7A,A′,B,B′).

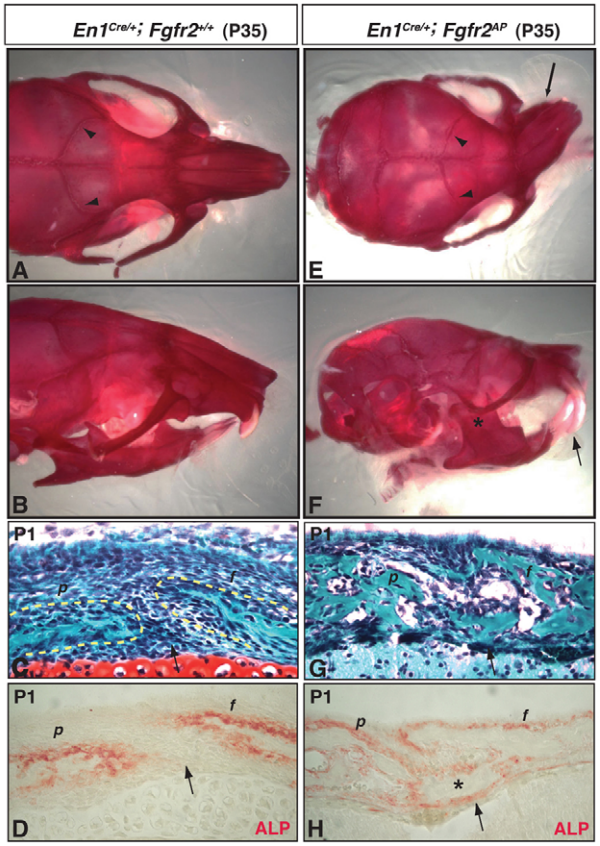

Fig. 6. Phenotypic consequences of $Fgfr2^{AP}$ allele activation in the *En1* lineage. (**A-H**) Whole-mount Alizarin Red staining (A,B,E,F), and histological analysis (C,D,G,H) from postnatal (P35) $En1^{Cre/+};Fgfr2^{+/+}$ and $En1^{Cre/+};Fgfr2^{AP}$ mice showing coronal synostosis (A,E, arrowheads; H, asterisk), severe distortion and malocclusion of the maxillary-premaxillary skeleton (E,F, arrows), and hypoplasia of the mandibular rudiment (F, asterisk) in $En1^{Cre/+};Fgfr2^{AP}$ mice. Histological sections, analyzed by trichrome staining (C,G) and for ALP activity in osteoblasts, demonstrate replacement of coronal suture mesenchyme by differentiated bone (D,H). Plane of section as A in Fig. 1J.

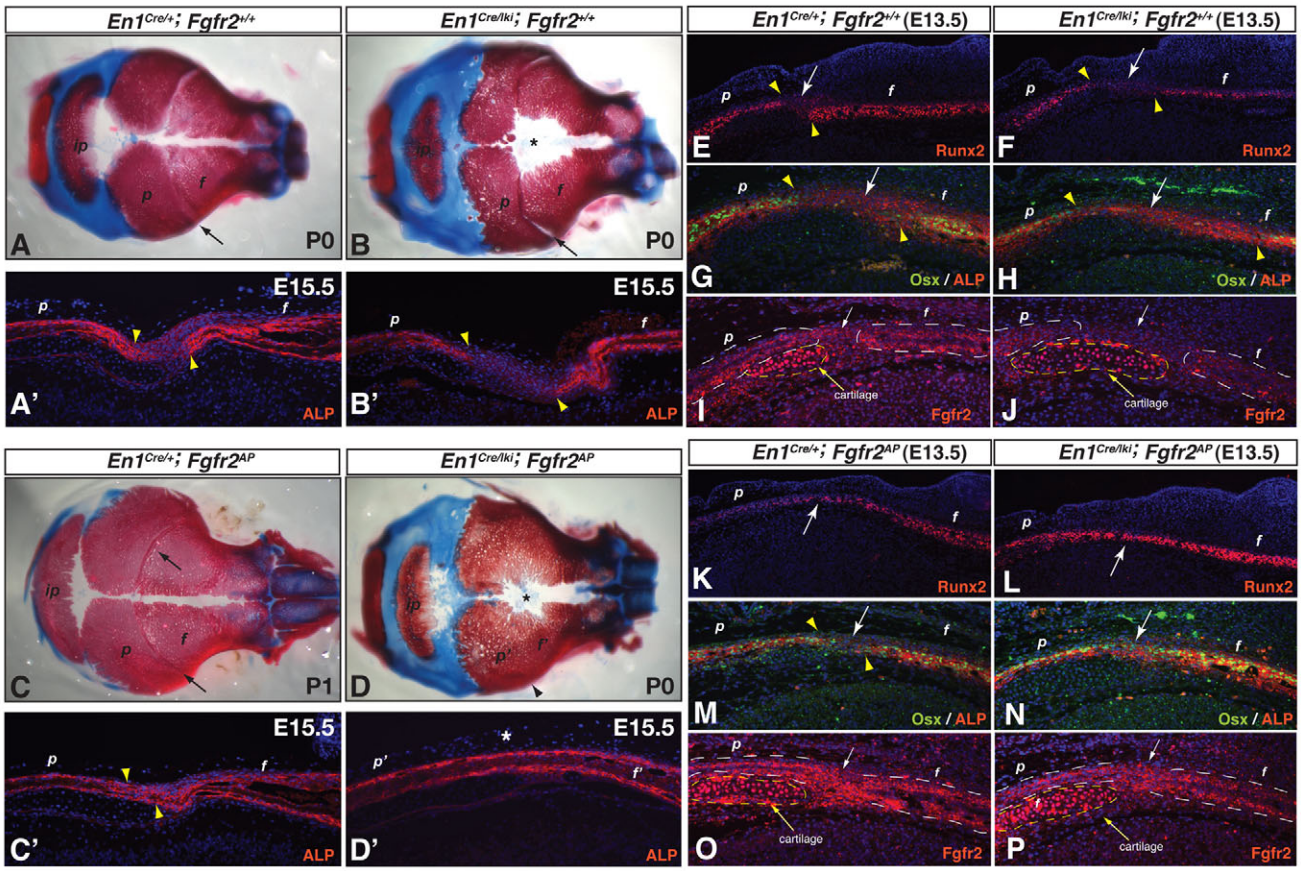

Fig. 7. *En1* interacts with Fgfr2 in regulating primordial calvarial osteogenesis and the establishment of the coronal suture. (**A-D′**) Whole-mount preparations (P0-P1) and histological analyses of ALP activity (E15.5) in calvaria of $En1^{Cre/+}$;$Fgfr2^{+/+}$, $En1^{Cre/Iki}$;$Fgfr2^{+/+}$, $En1^{Cre/+}$;$Fgfr2^{AP}$ and $En1^{Cre/Iki}$;$Fgfr2^{AP}$ mice. In contrast to $En1^{Cre/Iki}$;$Fgfr2^{+/+}$ mice, which exhibit ossification deficiencies, frontal foramina (B, asterisk) and increased coronal suture patency, $En1^{Cre/+}$;$Fgfr2^{AP}$ mice display coronal suture synostosis at birth (C, arrows), which is preceded by precocious osteogenic differentiation and narrowing of the sutural gap (C′, arrowheads indicate parietal-frontal bone edges). Strikingly, the coronal suture is absent in compound $En1^{Cre/Iki}$;$Fgfr2^{AP}$ mutants (D,D′). Section plane as B in Fig. 1J. (D′) p′ and f′ indicate presumptive parietal and frontal domains. (**E-P**) Comparative immunohistochemical analyses of osteogenic and sutural markers (Runx2, Osx, ALP and Fgfr2) in $En1^{Cre/+}$;$Fgfr2^{+/+}$ (E,G,I), $En1^{Cre/Iki}$;$Fgfr2^{+/+}$ (F,H,J), $En1^{Cre/+}$;$Fgfr2^{AP}$ (K,M,O) and $En1^{Cre/Iki}$;$Fgfr2^{AP}$ (L,N,P) mice at E13.5. Nuclear staining of $Runx2^+$ or Osx^+ cells is visible in red or green, respectively. ALP^+ cells are visible in red (G,H,M,N). $Fgfr2^+$ cells are visible in red, where white dashed lines demarcate the frontal/parietal osteogenic domains (I,J,O,P). White arrows indicate prospective sutural mesenchyme and yellow arrowheads demarcate the limits of the parietal and frontal anlagen, where discernible. Section plane as in Fig. 1I.

Surprisingly, rather than rescuing the $En1^{-/-}$ suture phenotype, *Fgfr2* activation leads to the complete absence of a morphologically discernible coronal suture in *En1*-null ($En1^{Cre/Iki}$;$Fgfr2^{AP}$) mice (Fig. 7D,D′), which is a more extreme phenotype than that observed in prototypical Apert ($En1^{Cre/+}$;$Fgfr2^{AP}$) mice expressing *En1* (Fig. 7C,C′). Corroborating the morphological data, analysis of early osteogenic markers shows that *En1*-null;$Fgfr2^{AP}$ mutants manifest ectopic activation of Runx2 and its downstream target Osx within cells of the prospective coronal suture mesenchyme by E13.5 (compare Fig. 7E-H with 7L,N). This phenotype is distinct from that of $En1^{Cre/+}$;$Fgfr2^{AP}$ embryos, in which discrete frontal and parietal osteogenic populations, separated by Osx-negative mesenchyme, merge only during the advanced stages of calvarial bone formation (Fig. 6G,H, Fig. 7C,C′,K,M). Interestingly, this *Osx*-negative sutural population is partially maintained in $En1^{Cre/+}$;$Fgfr2^{AP}$ embryos despite exaggerated levels of Fgfr2 protein in adjacent populations (Fig. 7O). By contrast, these *Osx*-negative mid-suture cells are absent from *En1*-null;$Fgfr2^{AP}$ embryos at E13.5. Hence, our data suggest an early necessary role for *En1* in conferring coronal suture identity and modulating its sensitivity to subsequent Fgfr2-mediated signals.

DISCUSSION

The cephalic origins of the coronal suture and frontal bone

Fate mapping the vertebrate cephalic mesoderm has presented a challenging problem in biology. In contrast to the somitic mesoderm, which displays distinct physical and molecular metamerism and fate-specific intraregionalization, the cephalic mesoderm presents no overt architectural organization and a scarcity of specific molecular identifiers (Noden and Trainor, 2005). By employing a novel strategy for fate mapping non-NeuC components of the mouse skull, the present study makes several important observations. First, we demonstrate that significant populations of calvarial mesenchyme arise from Hh-responsive $Gli1^+$ cells in the cephalic paraxial mesoderm, immediately adjacent to the neural tube. Inducing *Gli1-CreER*^{T2}-mediated

recombination between E7.5 and E8.0 conclusively shows that *Gli1*-expressing cells in the Mes give rise to the coronal sutures. In addition, we demonstrate that fate-mapped *Gli1-CreER^{T2}* cells also give rise to other dermatocranial structures of purported mesodermal origin, consistent with previous *Mesp1-Cre* lineage studies (Yoshida et al., 2008). Owing to the contiguous expression of *Gli1* along the length of the notochord we cannot ascertain the precise axial (anterior-posterior) origin of calvarial precursors; however, the cephalic distribution of *Gli1*$^{+}$ descendants at E9.5 suggests that these emanate from near the rostral mesencephalon and caudal diencephalon, in agreement with fate-mapping studies in chick (Evans and Noden, 2006).

Second, our short-term fate-mapping experiments in *Gli1-CreER^{T2};R26R* embryos indicate that Mes-derived calvarial precursors rapidly move from their axial positions to relocate laterally in the supraorbital region by E8.5-9.0, a trajectory that is consistent with DiI-labeling studies undertaken previously (Trainor et al., 1994; Trainor and Tam, 1995; Jiang et al., 2002). In agreement with rapid migratory dynamics, attempts to induce recombination by TM administration at later time points (after E8.0) yielded very little labeling in calvarial structures (data not shown), suggesting that transcriptional activation of *Gli1* in mesodermal cranial vault precursors is transient, and that these cells promptly escape the range of Hh signaling between E8.0 and E9.0. Interestingly, the recent identification of genetic lesions in *RAB23* and *IHH* in humans has implicated the involvement of Hh signaling in craniosynostosis pathophysiology (Jenkins et al., 2007; Klopocki et al., 2011). Although correlative studies in mouse have suggested a functional role for Ihh at late stages of suture development (Lenton et al., 2011), our lineage-tracing strategies provide the opportunity for investigating whether Hh responsiveness in primordial sutural and osteogenic precursors is crucial for even earlier processes pertaining to cell migration, specification and patterning (E7.5-8.5).

Third, our studies show that the frontal bone, despite being derived primarily from NeuC, receives significant *Gli1*-derived mesodermal lineage contributions, which can be traced to early intermingling with NeuC-derived cells above the developing eye. Although unanticipated, this finding is further substantiated by the observation of *Mesp1-Cre*-derived cells in the frontal bone. The evolutionary and heritable origins of the frontal bone have been a matter of contentious debate; in avians, the emerging view posits a dual Mes-NeuC contribution to this anlagen (Noden and Trainor, 2005; Evans and Noden, 2006), whereas prior analyses of the *Wnt1-Cre* and *Mesp1-Cre* lineages have claimed that its mammalian analog is derived exclusively from NeuC (Jiang et al., 2002; Yoshida et al., 2008). Our data, showing Mes-derived cells distributed within the caudal portion of the frontal bone, reconciles these two views and provides evidence that certain morphogenetic mechanisms have been largely conserved during mammalian and avian skull evolution. Nevertheless, these findings support a conceptual modification in our understanding of the Mes/NeuC lineage boundary. Although the NeuC compartment is precisely and stably delineated by the coronal suture mesenchyme, this boundary remains pervious to Mes and suggests that Mes-NeuC tissue interactions are more complex than previously thought.

Modeling cranial bone and coronal suture morphogenesis

The majority of studies on early phases of craniofacial development have focused on the behavior of migratory NeuC cells and their overall contribution to the skull rudiments (Noden, 1984; Le Douarin et al., 1993; Jiang et al., 2002). More recently, direct DiI tracing methods have documented the basal-to-apical movement of both frontal and parietal osteogenic precursors labeled at E13.5 (Yoshida et al., 2008; Ting et al., 2009). Expanding on these studies, our current *Gli1-CreER^{T2}* and *En1-CreER^{T1}* lineage analyses provide strong evidence that, prior to their migration, Mes- and NeuC-derived osteogenic precursors coalesce within the supraorbital domain between E10.5 and E11.5. Although our data agree with the reported apical migratory patterns assumed by osteogenic precursors after E13.5, we demonstrate that for the frontal bone this process is preceded by an earlier phase of caudal-to-rostral expansion (E11.5-12.5; Fig. 4V). Moreover, the precocious apical spread of osteogenic cells observed in the frontal bone of *En1*-null mutants suggests that this secondary migratory phase is tightly regulated by persistent *En1* transcription. Concurrently, we noted that whereas both *En1-Cre* and *Gli1-Cre* commonly label the suture and rostral portion of the parietal bone, the caudal domain of this osteogenic rudiment is labeled solely by *Gli1-Cre*. These observations argue for the existence of two distinct parietal progenitor populations. One emanates apically from a domain caudal to *En1* expression (Fig. 2J and our unpublished observations), which is similarly visualized by DiI labeling at E13.5 (Ting et al., 2009). However, we propose that the rostral portion of the parietal bone originates from the caudal *En1*$^{+}$ domain, which migrates apically in conjunction with sutural cells at an earlier phase (E11.5-12.5). The prior DiI labeling experiments failed to capture these *En1-Cre*-marked parietal progenitors because initial dye injections were performed after the cells had exited the supraorbital domain.

Similarly, the failure of DiI injections to label the coronal suture proper, in spite of effective marking of osteogenic populations (Yoshida et al., 2008; Ting et al., 2009), is likely to be due to the apical exit of sutural progenitors from the supraorbital domain prior to E13.5. Our data indicate that suture morphogenesis can be traced to considerably earlier stages of calvarial development (E10.5-12.5), preceding the elaboration of adjacent skeletal rudiments. We posit a model whereby coronal suture development ensues through the clonal and basal-to-apical trajectory of precursors arising from *En1*$^{+}$ mesoderm-derived cells within the supraorbital domain at E10.5 (Fig. 4V). Exit of the sutural precursors from this domain is coincident with their downregulation of *En1* (E11.5-12.0). That these *En1*-derived cells assume a specific molecular signature (*En1*$^{-}$/*Runx2*^{low}/*Osx*^{neg}), further suggests that coronal suture precursors are allocated early in calvarial development as a unique mesenchymal population, distinct from *En1*$^{+}$/*Runx2*^{high}/*Osx*^{high} osteoprogenitors. Of clinical relevance, our findings are consistent with recent etiological data indicating that craniosynostosis is an early (E12.5-13.5) development defect (Ting et al., 2009; Yen et al., 2010), but demonstrate that dysregulation of suture morphogenesis may initiate at even earlier stages (E10.5-11.5) than suggested in prior reports.

En1 is a regulator of the Mes/NeuC boundary and coronal suture specification

Collectively, our results provide genetic evidence suggesting that primordial cranial bone and suture morphogenesis is regulated by a supraorbital regulatory center, which is established across the Mes/NeuC lineage boundary between E10.5 and E11.5. Lineage boundary-associated tissue organizers direct compartmentalization, cell sorting, migration and signaling in both vertebrates and invertebrates (Dahmann et al., 2011). Cross-species studies suggest that Engrailed serves an evolutionarily conserved function in the formation or maintenance of heritable tissue compartments and their

associated boundaries (Irvine and Rauskolb, 2001; Dahmann et al., 2011). In comparison to the well-established roles of *Drosophila engrailed* in regulating lineage boundaries in insects (Blair and Ralston, 1997), analogous functions in vertebrates have been more difficult to assign. Straddling the mid-hindbrain, *En1* is likely to regulate segregation of mesencephalic and rhombencephalic lineages; however, because it is also required for the full elaboration of mid-hindbrain structures, assessment of its role in lineage segregation has proven difficult (Wurst et al., 1994). In the embryonic limb ectoderm, *En1* is required for normal maturation and maintenance of a sharp dorsal-ventral lineage boundary within the epithelium of the apical ectodermal ridge (Loomis et al., 1996; Kimmel et al., 2000). *En1* also regulates dorsal-ventral limb patterning in part through complex indirect interactions with *Lmx1b*, a transcription factor that demarcates a lineage compartment within the dorsal mesenchyme of the limb (Chen and Johnson, 2002; Qiu et al., 2009). Curiously, in addition to their limb patterning defects, *Lmx1b* mutants manifest a robust ablation of multiple cranial sutures (Chen et al., 1998), which raises the possibility that *En1* and *Lmx1b* might also interact during skull development.

Our findings illustrate a novel role for *En1* in the positioning and maintenance of a lineage boundary within the cephalic mesenchyme; loss of *En1* results in a caudal shift of the calvarial Mes/NeuC lineage boundary and incorporation of NeuC derivatives into definitive Mes territory (coronal suture mesenchyme and parietal bone). Consistent with these observations, *En1* mutants also exhibit perturbations in *Twist1* and *Msx2* expression, which are known regulators of the Mes/NeuC boundary (Merrill et al., 2006; Ting et al., 2009). It is therefore likely that *En1* plays a role in regulating early *Twist1* and *Msx2* expression, which in turn restricts the invasion of NeuC cells into definitive Mes-derived structures.

In addition to modulating coronal suture patterning, our study provides genetic evidence that *En1* interacts with *Fgfr2* in regulating the differentiation state of cranial osteogenic and sutural progenitors. Consistent with perturbed cranial osteogenesis, *En1*-null mutants exhibit diminished levels of Fgfr2 protein within calvarial bone anlagen, and restoration of Fgfr2 (through $Fgfr2^{AP}$ allele activation) results in partial correction of the bone formation defect. We therefore postulate that *En1* acts upstream of *Fgfr2* in promoting osteogenic differentiation (Fig. 8). Unexpectedly, our study reveals a novel role for *En1* in regulating primordial sutural specification and/or differentiation. In the presence of En1 protein, activation of $Fgfr2^{AP}$ results in late-phase coronal synostosis (E16.5-P1), which is in full agreement with prior reports (Chen et al., 2003; Holmes et al., 2009). By contrast, expression of $Fgfr2^{AP}$ in the absence of *En1* results in the inappropriate conversion of $ALP^{low}/Runx2^{low}/Osx^{-}$ sutural progenitors to cells exhibiting an osteogenic phenotype ($ALP^{high}/Runx2^{+}/Osx^{+}$), thus precluding the initial phases of coronal suture formation (E12.5-13.5). One possibility is that loss of *En1*, causing perturbations to the Mes/NeuC boundary and sutural morphogenesis, results in spatial misplacement of $Fgfr2^{AP}$-expressing cells outside of the expected Fgfr2 domains. It remains unknown, however, whether *Fgfr2* plays a further role in regulating the Mes/NeuC boundary and how this phenomenon per se affects coronal suture integrity. Alternatively, as *En1* expression normally extinguishes within sutural progenitors preceding their apical positioning (~E12), we postulate that the observed phenotype is due to an early requirement for *En1* in specifying sutural precursors and altering their susceptibility to Fgfr2 signals. It is also likely that downregulation of *Twist1* in the *En1*-null background contributes to the exacerbated sutural phenotype, as this transcription factor has been shown to regulate suture patency in part through *Fgfr2* (Connerney et al., 2006; Connerney et al., 2008).

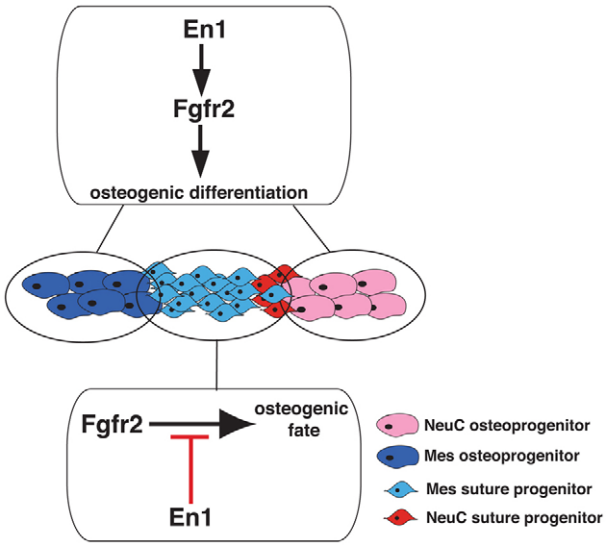

Fig. 8. Model for regulatory interactions between *En1* and *Fgfr2* during cranial osteogenesis and coronal suture formation. In the frontal and parietal bone anlagen, *En1* is required for normal expression levels of *Fgfr2*, which in turn induces osteogenic commitment and differentiation. Within the primordial coronal suture, *En1* plays a negative role in preventing precocious *Fgfr2*-mediated differentiation of the sutural mesenchyme.

We postulate that future assessment of these questions cannot be evaluated by simple in vitro methods, but rather must be examined within the context of temporal and spatial restrictions unique to the primordial coronal suture microenvironment. Our fate-mapping data suggest new strategies for attaining lineage-specific loss- and gain-of-function models for evaluating compartmental cell sorting and differential responsiveness to signaling cues, as shown to occur in epithelial boundaries (Dahmann et al., 2011). Of relevance to evolutionary studies, it is interesting that the frontal bone in birds forms from both the Mes and NeuC lineages without generating a coronal suture (Le Lievre, 1978; Noden and Trainor, 2005; Evans and Noden, 2006). The apparent recapitulation of this phenotype in *En1*-null;$Fgfr2^{AP}$ compound mutant mice offers opportunities for examining the molecular mechanisms underlying mammalian-avian species diversity. Future investigation of these crucial pathways during the primordial stages of coronal suture development should prove useful for the discovery of cell-based therapies for the treatment of a variety of skeletal disorders.

Acknowledgements
We thank Dr Alexandra Joyner for use of mouse strains and early guidance; Drs Mark Zervas and David Pechar for technical assistance and intellectual discussions concerning genetic fate mapping; Drs Deborah Yelon, Mayla Hsu and Isaac Brownell for critical reading of the manuscript; Drs Irma Thesleff (Helsinki, Finland) and Hyun-Mo Ryoo (Kyangpook, Korea) for the use of *Twist1* and *Runx2* riboprobes; and the NYU Histopathology Core for their excellent technical assistance.

Funding
This work was partially supported by the National Institutes of Health [AR051358 from NIAMS to C.B.] and by the Hirschl Charitable Trust Award [to C.A.L.]. The NYU Histopathology Core receives support from the Cancer Institute Center Support Grant [5 P30CA16087-31]. Deposited in PMC for release after 12 months.

Competing interests statement
The authors declare no competing financial interests.

Supplementary material
Supplementary material available online at
http://dev.biologists.org/lookup/suppl/doi:10.1242/dev.076729-/DC1

References

Ahn, S. and Joyner, A. L. (2004). Dynamic changes in the response of cells to positive hedgehog signaling during mouse limb patterning. *Cell* **118**, 505-516.
Araki, I. and Nakamura, H. (1999). Engrailed defines the position of dorsal di-mesencephalic boundary by repressing diencephalic fate. *Development* **126**, 5127-5135.
Blair, S. S. and Ralston, A. (1997). Smoothened-mediated Hedgehog signalling is required for the maintenance of the anterior-posterior lineage restriction in the developing wing of Drosophila. *Development* **124**, 4053-4063.
Chai, Y., Jiang, X., Ito, Y., Bringas, P., Jr, Han, J., Rowitch, D. H., Soriano, P., McMahon, A. P. and Sucov, H. M. (2000). Fate of the mammalian cranial neural crest during tooth and mandibular morphogenesis. *Development* **127**, 1671-1679.
Chen, H. and Johnson, R. L. (2002). Interactions between dorsal-ventral patterning genes lmx1b, engrailed-1 and wnt-7a in the vertebrate limb. *Int. J. Dev. Biol.* **46**, 937-941.
Chen, H., Ovchinnikov, D., Pressman, C. L., Aulehla, A., Lun, Y. and Johnson, R. L. (1998). Multiple calvarial defects in lmx1b mutant mice. *Dev. Genet.* **22**, 314-320.
Chen, L., Li, D., Li, C., Engel, A. and Deng, C. X. (2003). A Ser252Trp substitution in mouse fibroblast growth factor receptor 2 (Fgfr2) results in craniosynostosis. *Bone* **33**, 169-178.
Connerney, J., Andreeva, V., Leshem, Y., Muentener, C., Mercado, M. A. and Spicer, D. B. (2006). Twist1 dimer selection regulates cranial suture patterning and fusion. *Dev. Dyn.* **235**, 1345-1357.
Connerney, J., Andreeva, V., Leshem, Y., Mercado, M. A., Dowell, K., Yang, X., Lindner, V., Friesel, R. E. and Spicer, D. B. (2008). Twist1 homodimers enhance FGF responsiveness of the cranial sutures and promote suture closure. *Dev. Biol.* **318**, 323-334.
Couly, G. F., Coltey, P. M. and Le Douarin, N. M. (1993). The triple origin of skull in higher vertebrates: a study in quail-chick chimeras. *Development* **117**, 409-429.
Dahmann, C. and Basler, K. (1999). Compartment boundaries: at the edge of development. *Trends Genet.* **15**, 320-326.
Dahmann, C. and Basler, K. (2000). Opposing transcriptional outputs of Hedgehog signaling and engrailed control compartmental cell sorting at the Drosophila A/P boundary. *Cell* **100**, 411-422.
Dahmann, C., Oates, A. C. and Brand, M. (2011). Boundary formation and maintenance in tissue development. *Nat. Rev. Genet.* **12**, 43-55.
Deckelbaum, R. A., Majithia, A., Booker, T., Henderson, J. E. and Loomis, C. A. (2006). The homeoprotein engrailed 1 has pleiotropic functions in calvarial intramembranous bone formation and remodeling. *Development* **133**, 63-74.
Echelard, Y., Epstein, D. J., St-Jacques, B., Shen, L., Mohler, J., McMahon, J. A. and McMahon, A. P. (1993). Sonic hedgehog, a member of a family of putative signaling molecules, is implicated in the regulation of CNS polarity. *Cell* **75**, 1417-1430.
El Ghouzzi, V., Le Merrer, M., Perrin-Schmitt, F., Lajeunie, E., Benit, P., Renier, D., Bourgeois, P., Bolcato-Bellemin, A. L., Munnich, A. and Bonaventure, J. (1997). Mutations of the TWIST gene in the Saethre-Chotzen syndrome. *Nat. Genet.* **15**, 42-46.
Evans, D. J. and Noden, D. M. (2006). Spatial relations between avian craniofacial neural crest and paraxial mesoderm cells. *Dev. Dyn.* **235**, 1310-1325.
Hanafusa, H., Torii, S., Yasunaga, T. and Nishida, E. (2002). Sprouty1 and Sprouty2 provide a control mechanism for the Ras/MAPK signalling pathway. *Nat. Cell Biol.* **4**, 850-858.
Hanks, M. C., Loomis, C. A., Harris, E., Tong, C. X., Anson-Cartwright, L., Auerbach, A. and Joyner, A. (1998). Drosophila engrailed can substitute for mouse Engrailed1 function in mid-hindbrain, but not limb development. *Development* **125**, 4521-4530.
Holmes, G., Rothschild, G., Roy, U. B., Deng, C. X., Mansukhani, A. and Basilico, C. (2009). Early onset of craniosynostosis in an Apert mouse model reveals critical features of this pathology. *Dev. Biol.* **328**, 273-284.
Hopman, A. H., Ramaekers, F. C. and Speel, E. J. (1998). Rapid synthesis of biotin-, digoxigenin-, trinitrophenyl-, and fluorochrome-labeled tyramides and their application for In situ hybridization using CARD amplification. *J. Histochem. Cytochem.* **46**, 771-777.
Hui, C. C., Slusarski, D., Platt, K. A., Holmgren, R. and Joyner, A. L. (1994). Expression of three mouse homologs of the Drosophila segment polarity gene cubitus interruptus, Gli, Gli-2, and Gli-3, in ectoderm- and mesoderm-derived tissues suggests multiple roles during postimplantation development. *Dev. Biol.* **162**, 402-413.
Irvine, K. D. and Rauskolb, C. (2001). Boundaries in development: formation and function. *Annu. Rev. Cell Dev. Biol.* **17**, 189-214.
Jabs, E. W., Muller, U., Li, X., Ma, L., Luo, W., Haworth, I. S., Klisak, I., Sparkes, R., Warman, M. L. and Mulliken, J. B. (1993). A mutation in the homeodomain of the human MSX2 gene in a family affected with autosomal dominant craniosynostosis. *Cell* **75**, 443-450.
Jenkins, D., Seelow, D., Jehee, F. S., Perlyn, C. A., Alonso, L. G., Bueno, D. F., Donnai, D., Josifova, D., Mathijssen, I. M., Morton, J. E. et al. (2007). RAB23 mutations in Carpenter syndrome imply an unexpected role for hedgehog signaling in cranial-suture development and obesity. *Am. J. Hum. Genet.* **80**, 1162-1170.
Jiang, X., Iseki, S., Maxson, R. E., Sucov, H. M. and Morriss-Kay, G. M. (2002). Tissue origins and interactions in the mammalian skull vault. *Dev. Biol.* **241**, 106-116.
Kiecker, C. and Lumsden, A. (2005). Compartments and their boundaries in vertebrate brain development. *Nat. Rev. Neurosci.* **6**, 553-564.
Kimmel, R. A., Turnbull, D. H., Blanquet, V., Wurst, W., Loomis, C. A. and Joyner, A. L. (2000). Two lineage boundaries coordinate vertebrate apical ectodermal ridge formation. *Genes Dev.* **14**, 1377-1389.
Klopocki, E., Lohan, S., Brancati, F., Koll, R., Brehm, A., Seemann, P., Dathe, K., Stricker, S., Hecht, J., Bosse, K. et al. (2011). Copy-number variations involving the IHH locus are associated with syndactyly and craniosynostosis. *Am. J. Hum. Genet.* **88**, 70-75.
Le Douarin, N. M., Ziller, C. and Couly, G. F. (1993). Patterning of neural crest derivatives in the avian embryo: in vivo and in vitro studies. *Dev. Biol.* **159**, 24-49.
Le Lievre, C. S. (1978). Participation of neural crest-derived cells in the genesis of the skull in birds. *J. Embryol. Exp. Morphol.* **47**, 17-37.
Lenton, K., James, A. W., Manu, A., Brugmann, S. A., Birker, D., Nelson, E. R., Leucht, P., Helms, J. A. and Longaker, M. T. (2011). Indian hedgehog positively regulates calvarial ossification and modulates bone morphogenetic protein signaling. *Genesis* **49**, 784-796.
Lenton, K. A., Nacamuli, R. P., Wan, D. C., Helms, J. A. and Longaker, M. T. (2005). Cranial suture biology. *Curr. Top. Dev. Biol.* **66**, 287-328.
Li, C., Scott, D. A., Hatch, E., Tian, X. and Mansour, S. L. (2007). Dusp6 (Mkp3) is a negative feedback regulator of FGF-stimulated ERK signaling during mouse development. *Development* **134**, 167-176.
Loomis, C. A., Harris, E., Michaud, J., Wurst, W., Hanks, M. and Joyner, A. L. (1996). The mouse Engrailed-1 gene and ventral limb patterning. *Nature* **382**, 360-363.
Merrill, A., Bochukova, E., Brugger, S., Ishii, M., Pilz, D., Wall, S., Lyons, K., Wilkie, A. and Maxson, R. J. (2006). Cell mixing at a neural crest-mesoderm boundary and deficient ephrin-Eph signaling in the pathogenesis of craniosynostosis. *Hum. Mol. Genet.* **15**, 1319-1328.
Morriss-Kay, G. M. and Wilkie, A. O. (2005). Growth of the normal skull vault and its alteration in craniosynostosis: insights from human genetics and experimental studies. *J. Anat.* **207**, 637-653.
Nagata, M., Nuckolls, G. H., Wang, X., Shum, L., Seki, Y., Kawase, T., Takahashi, K., Nonaka, K., Takahashi, I., Noman, A. A. et al. (2010). The primary site of the acrocephalic feature in Apert Syndrome is a dwarf cranial base with accelerated chondrocytic differentiation due to aberrant activation of the FGFR2 signaling. *Bone* **48**, 847-856.
Noden, D. M. (1984). Craniofacial development: new views on old problems. *Anat. Rec.* **208**, 1-13.
Noden, D. M. and Trainor, P. A. (2005). Relations and interactions between cranial mesoderm and neural crest populations. *J. Anat.* **207**, 575-601.
Qiu, Q., Chen, H. and Johnson, R. L. (2009). Lmx1b-expressing cells in the mouse limb bud define a dorsal mesenchymal lineage compartment. *Genesis* **47**, 224-233.
Rice, D. P., Aberg, T., Chan, Y., Tang, Z., Kettunen, P. J., Pakarinen, L., Maxson, R. E. and Thesleff, I. (2000). Integration of FGF and TWIST in calvarial bone and suture development. *Development* **127**, 1845-1855.
Roybal, P. G., Wu, N. L., Sun, J., Ting, M. C., Schafer, C. A. and Maxson, R. E. (2010). Inactivation of Msx1 and Msx2 in neural crest reveals an unexpected role in suppressing heterotopic bone formation in the head. *Dev. Biol.* **343**, 28-39.
Sgaier, S. K., Millet, S., Villanueva, M. P., Berenshteyn, F., Song, C. and Joyner, A. L. (2005). Morphogenetic and cellular movements that shape the mouse cerebellum; insights from genetic fate mapping. *Neuron* **45**, 27-40.
Shen, H., Wilke, T., Ashique, A. M., Narvey, M., Zerucha, T., Savino, E., Williams, T. and Richman, J. M. (1997). Chicken transcription factor AP-2: cloning, expression and its role in outgrowth of facial prominences and limb buds. *Dev. Biol.* **188**, 248-266.
Soriano, P. (1999). Generalized lacZ expression with the ROSA26 Cre reporter strain. *Nat. Genet.* **21**, 70-71.
Speel, E. J., Hopman, A. H. and Komminoth, P. (1999). Amplification methods to increase the sensitivity of in situ hybridization: play card(s). *J. Histochem. Cytochem.* **47**, 281-288.
Ting, M. C., Wu, N. L., Roybal, P. G., Sun, J., Liu, L., Yen, Y. and Maxson, R. E., Jr (2009). EphA4 as an effector of Twist1 in the guidance of osteogenic

precursor cells during calvarial bone growth and in craniosynostosis. *Development* **136**, 855-864.
Trainor, P. A. and Tam, P. P. (1995). Cranial paraxial mesoderm and neural crest cells of the mouse embryo: co-distribution in the craniofacial mesenchyme but distinct segregation in branchial arches. *Development* **121**, 2569-2582.
Trainor, P. A., Tan, S. S. and Tam, P. P. (1994). Cranial paraxial mesoderm: regionalisation of cell fate and impact on craniofacial development in mouse embryos. *Development* **120**, 2397-2408.
Wang, Y., Xiao, R., Yang, F., Karim, B. O., Iacovelli, A. J., Cai, J., Lerner, C. P., Richtsmeier, J. T., Leszl, J. M., Hill, C. A. et al. (2005). Abnormalities in cartilage and bone development in the Apert syndrome FGFR2(+/S252W) mouse. *Development* **132**, 3537-3548.
Wilkie, A. O. (1997). Craniosynostosis: genes and mechanisms. *Hum. Mol. Genet.* **6**, 1647-1656.
Wurst, W., Auerbach, A. B. and Joyner, A. L. (1994). Multiple developmental defects in Engrailed-1 mutant mice: an early mid-hindbrain deletion and patterning defects in forelimbs and sternum. *Development* **120**, 2065-2075.
Yen, H. Y., Ting, M. C. and Maxson, R. E. (2010). Jagged1 functions downstream of Twist1 in the specification of the coronal suture and the formation of a boundary between osteogenic and non-osteogenic cells. *Dev. Biol.* **347**, 258-270.
Yoshida, T., Vivatbutsiri, P., Morriss-Kay, G., Saga, Y. and Iseki, S. (2008). Cell lineage in mammalian craniofacial mesenchyme. *Mech. Dev.* **125**, 797-808.
Zervas, M., Millet, S., Ahn, S. and Joyner, A. L. (2004). Cell behaviors and genetic lineages of the mesencephalon and rhombomere 1. *Neuron* **43**, 345-357.